J. Membrane Biol. 155, 35–45 (1997)

The Journal of
Membrane
Biology

Hyperpolarization-activated Ca^{2+}-permeable Channels in the Plasma Membrane of Tomato Cells

A. Gelli, E. Blumwald
Department of Botany, University of Toronto, 25 Willcocks Street, Toronto, Ontario CANADA M5S 3B2

Received: 13 February 1996/Revised: 12 August 1996

Abstract. The hyperpolarization of the electrical plasma membrane potential difference has been identified as an early response of plant cells to various signals including fungal elicitors. The hyperpolarization-activated influx of Ca^{2+} into tomato cells was examined by the application of conventional patch clamp techniques. In both whole cell and single-channel recordings, clamped membrane voltages more negative than −120 mV resulted in time- and voltage-dependent current activation. Single-channel currents saturated with increasing activities of Ca^{2+} and Ba^{2+} from 3 to 26 mM and the single channel conductance increased from 4 pS to 11 pS in the presence of 20 mM Ca^{2+} or Ba^{2+}, respectively. These channels were 20–25 and 10–13 times more permeable to Ca^{2+} than to K^+ and to Cl^-, respectively. Channel currents were strongly inhibited by 10 μM lanthanum and 50% inhibited by 100 μM nifedipine. This evidence suggests that hyperpolarization-activated Ca^{2+}-permeable channels provide a mechanism for the influx of Ca^{2+} into tomato cells.

Key words: Tomato protoplasts — Patch clamp — Calcium channels — Hyperpolarized electrical membrane potential differences — Signal transduction

Introduction

Changes in the electrical potential difference across the plasma membrane of higher plants have been shown to be among the most rapid alterations induced by abiotic (Assmann, Simoncini & Schroeder, 1985; Serrano, Zeiger & Hagiwara, 1988) and biotic stresses (Felle, 1988; Ullrich & Novacky, 1991; Lohse & Hedrich 1992). The sensitivity of the electrical membrane potential to different stimuli suggests that the electrogenic exchange of ions across the plasma membrane could serve for the transduction of signals (i.e., pathogen elicitors) perceived at the plasma membrane. The hyperpolarization of the electrical plasma membrane potential difference has been identified as an early response of plant cells to blue and red light (Shimazaki, Kinoshita & Nishimura, 1980; Assmann et al., 1985; Serrano et al., 1988), auxins (Felle, 1988), the fungal toxin fusicoccin (Marre, 1985) and specific fungal elicitors (Vera-Estrella et al., 1994). The treatment of tomato cell suspension cultures with specific fungal elicitors led to a guanine nucleotide binding protein (G-protein)-mediated dephosphorylation of the host plasma membrane H^+-ATPase. This resulted in the stimulation of the H^+-pump activity with the concomitant hyperpolarization of the electrical potential difference across the plasma membrane and the acidification of the extracellular milieu (Vera-Estrella et al., 1994; Xing, Higgins & Blumwald, 1996). Thus a hyperpolarization-activated influx of Ca^{2+} into the host cell could provide a pathway for the elevation of cytosolic free Ca^{2+} concentrations that mediates the induction of several biochemical pathways that are part of the plant defense response (Ebel & Cosio, 1994). Many of the biochemical responses associated with the plant defense mechanisms are inhibited by the depletion of extracellular Ca^{2+} or stimulated in the presence of ionophores that allowed the entry of Ca^{2+} into the cells (Schwacke & Hager, 1992; Ebel & Cosio, 1994) suggesting that fluctuations in cytosolic Ca^{2+} are required for an effective defense response by the cell.

The earliest electrophysiological evidence for the operation of Ca^{2+}-permeable channels in the plasma membrane came from studies done in charophyte algae (Hayama, Shimmen & Tazawa, 1979; Lunevsky et al., 1983). Most of the studies on Ca^{2+} permeation through the plasma membrane of higher plants have shown the activation of Ca^{2+}-permeable channels at depolarized

Correspondence to: E. Blumwald

electrical membrane potential differences (Fairely-Grenot & Assmann, 1992; White, 1994; Huang Grunes & Kochian, 1994; Thuleau et al., 1994; Marshall et al., 1994; Piñeros & Tester, 1995) including an ABA-activated nonspecific Ca^{2+}-permeable channel (Schroeder & Hagiwara, 1990). Plasma membrane stretch-activated channels have also been reported as pathways for the influx of Ca^{2+} (Cosgrove & Hedrich, 1991; Ding & Pickard, 1993).

Recently, hyperpolarization-activated Ca^{2+} influx has been also reported (Stoeckel & Takeda, 1995). Although a full characterization of these currents has yet to be done, it appears that these channels are different from the putative depolarization-activated Ca^{2+} channels. Other reports have described hyperpolarization-activated nonselective cation channels that could also potentially provide a pathway for the influx of Ca^{2+} (Fairley, Laver & Walker, 1991; Cosgrove & Hedrich, 1991). The existence of hyperpolarization- and depolarization-activated Ca^{2+}-permeable channels in the plasma membrane may be a required feature that allows plant cells to efficiently couple the perception of stimuli at the plasma membrane to fluctuations in cytosolic Ca^{2+} concentrations.

In this report we present evidence for Ca^{2+} influx at hyperpolarized membrane potentials in the plasma membrane of tomato cells. These channels are voltage-dependently gated, selective for Ca^{2+} over K^+ and Cl^-, sensitive to inhibitors including La^{3+} and nifedipine and they provide a mechanism for the influx of Ca^{2+} into tomato cells.

Material and Methods

Plant Material

Cell suspensions of tomato (*Lycopersicon esculentum L.*) were grown in 500 ml Erlenmeyer flasks containing 90 ml of Murashige and Skoog medium (Vera-Estrella et al., 1994). The flasks were kept in the dark at 23°C on a rotary shaker (120 rpm) and subcultured weekly.

Isolation of Tomato Protoplasts

Protoplasts were prepared from 3-to-5-day-old cultured cells by digestion for 1.5 hr in digestion buffer (0.4 M sorbitol, 0.5 mM $CaCl_2$, 0.3 M Mes/KOH pH 5.5 with 2.0% cellulase (Seishin Corporation, Chuo-ku, Tokyo Japan), 0.5% BSA and 0.1% pectolyase (Seishin Corporation, Chuo-ku, Tokyo Japan). Digestion of cells was carried out in the dark at 30°C in a rotary shaker. The digested cells were filtered through Miracloth to remove all cell debris and the filtrate containing the protoplasts was centrifuged at 200 × *g* for 5 min. The protoplasts were resuspended in 10 ml of wash buffer (0.4 M sorbitol, 0.2 mM $CaCl_2$, 15 mM Tris-Mes pH 5.5) and collected after centrifugation at 200 × *g* for 5 min. This washing step was repeated twice. The protoplasts were loaded on top of a 0/25% discontinuous Percoll gradient and centrifuged at 250 × *g* for 20 min. Purified protoplasts were collected at the 0/25% Percoll interface. The protoplasts were resuspended in wash buffer and centrifuged at 200 × *g* for 5 min. This washing step was repeated twice.

Measurements of Whole-Cell Currents

Experiments were performed using conventional whole-cell and single-channel patch-clamp techniques (Hamill et al., 1981). Protoplasts were kept in a glass chamber containing 5, 10, 20, 35 or 50 mM $BaCl_2$ (or $CaCl_2$) as described in the legends to figures, 0.1 mM potassium glutamate, 1 mM $MgSO_4$, 5 mM Tris-Mes buffer (pH 7.1–7.3) and sorbitol to give a final osmolarity of 450 mosmol. Glass pipettes pulled with a vertical puller (Adams & List, New York) from borosilicate glass capillaries (Kimax-51, VWR, Boston, MA) coated with silicone (Sigmacote, Sigma) and fire polished, had a tip resistance of 5–10 MΩ when filled with (in mM): 100 potassium glutamate, 1 $MgSO_4$, 3 MgATP (freshly added to the pipette solution), 0.05 $CaCl_2$ + 0.10 BATA to give a final free Ca^{2+} concentration of 100 nM (Tsien, 1980), 5 mM Tris-Mes buffer (pH 6.1–6.3) and sorbitol with a final osmolarity of 475 mosmol.

The whole-cell configuration was initially obtained by forming a gigaseal with resistance of 6 to 8 GΩ in the cell-attached mode followed by the application of further suction to rupture the plasma membrane within the pipette tip. Whole-cell experiments were performed at 23°C in voltage-clamp mode using Dagan 3900 amplifier (Dagan Corporation, MA) digitized on line (TL-1 DMA Interface; Axon Instruments, Foster City, CA), stored on a 386 based 33 MHz computer and acquired and analyzed with pClamp 6.0.2 software (Axon Instruments). Voltage-pulse protocols were applied during data acquisition as described in the legends to figures. Tail current experiments were performed by activating inward currents with −160 mV pulses for 2.5 sec followed by a step up in voltage to −80 mV. This protocol was repeated 15 times with a subsequent increase in the deactivating pulse of 10 mV. All membrane potentials reported here have been corrected for liquid junction potentials (Barry & Lynch, 1991). Whole-cell currents were filtered at 500 Hz with a four-pole Bessel filter contained in the Dagan amplifier.

Voltage Dependence of Whole Cell Currents

To determine the voltage-dependency of channel gating, the relative conductance of whole cell currents was plotted as a function of the clamped electrical membrane potential difference and fit with the following Boltman term:

$$1n[1 - \theta\ (V)]/\theta(V) = \Delta G_i/RT + zFV/RT \qquad (1)$$

where the relative conductance (θ) is defined as the ratio G/G_{max}. The total free energy associated with the transition from the closed to the open state of a channel within an electric field is defined by two variables: the internal free energy of opening (ΔG_i) and the change in energy of the dipole moments (z) associated with the two conformational states of the channel protein in the electric field (Labarca, Coronado & Miller, 1980).

Measurements of Single-Channel Currents

For single-channel measurements, outside-out patches of plasma membrane were obtained after the whole-cell mode by quickly pulling the pipette away from the protoplasts. Both the bathing and the pipette solutions used in single channel measurements were the same as those used in whole-cell measurements. Single-channel currents were measured with the same equipment and computer software as that used in

whole-cell measurements. Data were filtered with a four-pole Bessel filter at 200 Hz, digitized at 2KHz and stored on disk.

Permeability ratios for solutions containing a mixture of monovalent and divalent ions were calculated from the constant field equations proposed by Goldman-Hodgkin-Katz (Lewis, 1979) where the reversal potential is determined by the zero current condition:

$$I_{K}^{+} + I_{Ca}^{2+} + I_{Cl}^{-} = 0 \quad (2)$$

In calculating channel selectivity when K^+, Ca^{2+} and Cl^- are permeant, it is necessary to measure two or more values of the reversal potential in two different solutions (*A* and *B*). The zero current equations for the two conditions can then be manipulated to calculate relative permeabilities: P_{Ca}^{2+}/P_{K}^{+}, P_{Cl}^{-}/P_{K}^{+} and P_{Ca}^{2+}/P_{Cl}^{-} (Hille, 1992; Allen & Sanders, 1995). The following equations were used to calculate permeability ratios:

$$P_{Ca}^{2+}/P_{K}^{+} = (Q_{Cl}^{A}Q_{K}^{B} - Q_{Cl}^{B}Q_{K}^{A})/(Q_{Cl}^{B}Q_{Ca}^{A} - Q_{Cl}^{A}Q_{Ca}^{B}) \quad (3)$$

$$P_{Cl}^{-}/P_{K}^{+} = -P_{Ca}^{2+}/P_{K}^{+}Q_{Ca}^{B} - Q_{K}^{B}/Q_{Cl}^{B} \quad (4)$$

where Q is defined as:

$$z^2 \frac{EF^2}{RT} \frac{[S]_i - [S]_0 e^{(-zEF/RT)}}{1 - e^{(-zEF/RT)}} \quad (5)$$

and where E is the reversal potential (in volts), F is the Faraday constant, R is the gas constant, T is the absolute temperature, z is the valency of the ion, S, [S] is the activity of the ion on the cytoplasmic ((*i*) pipette solution) and extracellular side ((*o*) bathing solution) of the plasma membrane and *A* and *B* are solutions with distinct ion concentrations. Ion concentrations were expressed as ion activities for all calculations of permeability ratios and Nernst potentials. Activities of ions were derived by using activity coefficients estimated from the Debye & Hückel equation (Nobel, 1991). For the measurement of whole-cell and single-channel currents Ba^{2+} was used as a Ca^{2+} analogue for several reasons: (i) Ba^{2+} blocks potassium channels in the plasma membrane of both animal (Armstrong & Taylor, 1980) and plant (Wegner, De Boer & Raschke, 1994) cells that could potentially mask Ca^{2+} currents; (ii) Ba^{2+} enhances the resolution of Ca^{2+} channels since the magnitude of the single channel currents are larger with Ba^{2+} as the charge carrier (Gelli & Blumwald, 1993).

The open and closed time constants were determined from exponential fittings of open and closed time histograms using pClamp software. Histogram fits were determined to be good only if the standard errors of time constants were less than 10% and if the criteria set by pClamp software (i.e., goodness of fit ≈2.0) was met. Mean open and closed times were determined by the method of Labacca et al (1980). Open channel probabilities (P_O) were calculated from the ratio of mean open time to the total recording time (mean open time + mean closed time). In this way values of N (total number of channels in the patch of membrane) estimated from single-channel records could not affect values of P_O since this method considered only the average number of channels in the open state. This is relevant for channels with low open state probabilities where the difficulty in determining N usually results in an underestimate (Plant, Gelli & Blumwald, 1994).

Results

Hyperpolarization-induced Influx of Ba^{2+} and Ca^{2+}

Whole cell currents were measured when the electrical potential difference across the plasma membrane of tomato protoplasts was clamped from −180 to 40 mV in increments of 20 mV from a holding potential of −60 mV. At this holding potential the probability of channel opening is very low, thus channel activation (open state) by hyperpolarizing-membrane potentials could be specifically studied. Only membrane voltages more negative than −120 mV (hyperpolarized membrane potentials) elicited large inward currents with Ba^{2+} as the charge carrier (Fig. 1*A*). Current activation was fast and followed an exponential time course. The voltage activation of the Ba^{2+} currents was time-dependent and the magnitude of the currents was largest at −180 mV. These currents were active at membrane voltages that were within the range of the Nernst potentials for K^+ (−167 mV) and Cl^- (−158 mV) suggesting that these currents were not due to the movement of K^+ or of Cl^-.

Similarly, replacing Ba^{2+} with Ca^{2+} on the extracellular side of the protoplasts resulted in inward currents elicited by hyperpolarized membrane voltages. These currents were time- and voltage-dependent. With Ca^{2+} as the change carrier, current activation was faster and the magnitude of the currents smaller (Fig. 1*B*). Activation of Ca^{2+} currents also followed an exponential time course. The nonlinear current-voltage relationship (Fig. 1*C*) revealed inward currents that were strongly voltage-dependent with maximum current activation only at hyperpolarized membrane potentials.

Whole cells were exposed to 50 mM Ca^{2+} while the membrane voltage was clamped from −200 to 100 mV for 1.2 sec (Fig. 1*D*). A fast voltage ramp increases the probability of measuring a large proportion of channels in a given open state. The same ramp experiment was done in the presence of 10 mM Ca^{2+} (*not shown*). As observed in Fig. 1*A* and *B*, inward currents were largest at negative membrane potentials that were within the range of the reversal potentials for K^+ and Cl^- suggesting that the voltage-activated currents were due to the movement of Ca^{2+} into the cell. The Ca^{2+} inward currents reversed direction at 35 mV in the presence of 50 mM Ca^{2+} and at 10 mV in the presence of 10 mM Ca^{2+} with tail current experiments (*not shown*). These reversal potentials suggest that all three ions (K^+, Cl^- and Ca^{2+}) are permeant however the change in the reversal potential toward the Nernst potential for Ca^{2+} (154 mV) indicates that the channel is more permeable to Ca^{2+} than to K^+ or Cl^-. Using these reversal potentials for the calculation of permeability ratios (*see* Material and Methods), a P_{Ca}^{2+}/P_{K}^{+} of about 20, a P_{Cl}^{-}/P_{K}^{+} of about 2 and a P_{Ca}^{2+}/P_{Cl}^{-} of about 10 weeks were obtained. Similar results were obtained with Ba^{2+} as the charge carrier (*not shown*).

To examine the voltage-dependency of channel gating a Boltman plot (Fig. 2) was constructed from whole cell recordings similar to those shown in Fig. 1. The gating charge (z), corresponding to the slope of the fit, revealed that both Ba^{2+} ($z = 1.09 \pm 0.15$) and Ca^{2+} ($z = 1.09 \pm 0.19$) currents were sensitive to the electric field

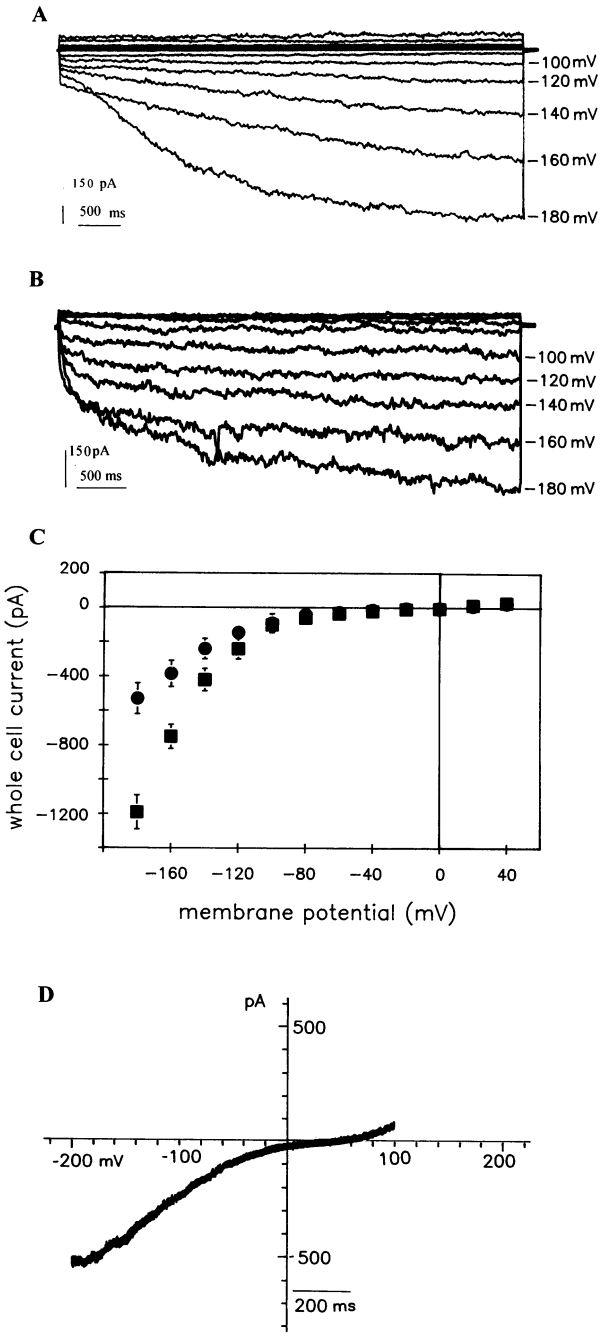

Fig. 1. Voltage-dependent Ba^{2+} and Ca^{2+} inward currents of tomato protoplasts. Inward currents across protoplasts were measured by clamping the membrane potential to −180 mV for a duration of 5 sec followed by a 20 mV increment from −180 to 40 mV from a holding potential of −60 mV. (*A*) Protoplasts bathed in 50 mM Ba^{2+} (100 nM free cytoplasmic calcium (pipette interior)) displayed time-dependent inward currents in response to negative membrane voltages. Largest current levels corresponded to the largest negative membrane voltage. (*B*) Replacing the protoplast's bathing solution of 50 mM Ba^{2+} with 50 mM Ca^{2+} revealed a similar type of voltage-dependent current however, the time-dependence of voltage-activation appeared to be faster with Ca^{2+} than with Ba^{2+}. (*C*) Current-voltage plot from protoplasts in *A* (■) and *B* (●). Current levels measured at 4.8 sec from the onset of the imposed voltage as described above were plotted against their respective voltages. Values are Mean ± SD ($n = 12$). (*D*) A voltage ramp from −200 to 100 mV in whole protoplasts. Similar results were observed in at least 12 other protoplasts.

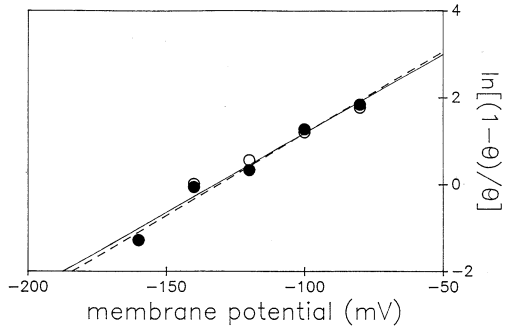

Fig. 2. A Boltzman plot of the whole-cell currents recorded in 50 mM of either Ba^{2+} (●) or Ca^{2+} (◎) in the bathing solution and with 100 nM cytoplasmic-free calcium in the pipette. The relative conductance (θ) is defined as the ratio of G/G_{max}. The gating charge (z) of the channel is represented by the slope of the least-squares fit line. The free-energy (kcal/mol) associated with the transition of the channel from the closed to the open state was determined from the Y-intercept (ΔG_i) of the plot. Values are Mean ± SD ($n = 12$). Error bars are smaller than symbol size.

across the plasma membrane, comparable to that of K^+ currents in the plasma membrane of xylem parenchyma cells ($z = 1.16 \pm 0.22$) (Wegner et al., 1992). The free energy (Gibbs free energy = ΔG_i) associated with the transition of the channel from the closed to the open state in the plasma membrane was similar for Ba^{2+} ($\Delta G_i = 2.92 \pm 0.23$ kcalmol^{-1}) and for Ca^{2+} ($\Delta G_i = 2.81 \pm 0.29$ kcalmol^{-1}).

Inhibition of Inward Currents by Nifedipine

The organic inhibitor nidefipine, known for its effectiveness in blocking L-type calcium channels in animal (Catteral & Striessnig, 1992, Hille, 1993) and Ca^{2+}-permeable channels in plant cells (Gelli & Blumwald, 1993; Allen & Sanders, 1994) was used here in an attempt to further characterize the inward currents. The half-blocking concentrations reported are within the range of 0.5 to 100 μM, depending on the type of cell (Hille, 1992). Inward currents were reduced by about 50% when 100 μM of nifedipine was added to the extracellular side (bathing chamber) of the protoplasts (Fig. 3). The external Ba^{2+} concentration was maintained at 50 mM. Whole-cell currents were recorded by applying voltage pulses from −180 mV in increments of 20 to 40

mV from a holding potential of −60 mV before (Fig. 3*A*) and after (Fig. 3*B*) the addition of nifedipine. The presence of nifedipine reduced whole cell currents and also slowed down current activation (Fig. 3*B*). The nonlinear current-voltage relationship (Fig. 3*C*) clearly demonstrated the reduction in whole cell currents by nifedipine. The block of whole cell currents was not strongly voltage-dependent as was shown by plotting the fraction of current inhibited by nifedipine as a function of the applied membrane voltage (Fig. 3*D*).

Voltage-dependent Ca^{2+} Currents at the Single-Channel Level

Single-channel currents were measured from outside-out patches of plasma membrane exposed to various concentrations of Ca^{2+} and Ba^{2+} (bathing solution) while polarizing the plasma membrane to membrane potentials from −120 to −190 mV. Single-channel recordings from isolated patches exposed to 50 mM Ca^{2+} revealed voltage-dependent channel activity (Fig. 4*A*) in that channel events became more frequent with increasingly negative membrane voltages. Channel activity was detected at membrane potentials corresponding to the reversal potentials of K^+ (−167 mV) and Cl^- (−158 mV) suggesting that the downward deflections corresponded to the movement of Ca^{2+}. Channel recordings at potentials greater than −190 mV were difficult to obtain since the isolated patch of membrane became very unstable at these large potential differences.

The current-voltage relationship constructed from single-channel recordings similar to those shown in Fig. 4*A* was ohmic (Fig. 4*B*) for all three concentrations of extracellular Ca^{2+} (5, 20 and 50 mM) (activities: 3.9, 13.3 and 26.1 mM). Least-squares analysis yielded reversal potentials of 14, 30 and 42 mV for channel currents recorded in the presence of 5, 20 and 50 mM, respectively. The reversal potential of the single-channel currents shifted toward the equilibrium potential for Ca^{2+} (≈+133 mV with 5 mM (extracellular) and 100 nM (cytoplasmic)) with increasing extracellular Ca^{2+} concentrations (Fig. 4*B*) suggesting that these channels are more permeable to Ca^{2+} than to K^+ or Cl^-. Based on the reversal potentials, permeability ratios (P^{2+}_{Ca}/P^{+}_{K}, P^{-}_{Cl}/P^{+}_{K} and P^{2+}_{Ca}/P^{-}_{Cl}) revealed that these channels are about 25 times more permeable to Ca^{2+} than to K^+, 13 times more permeable to Ca^{2+} than to Cl^- and 2 times more permeable to Cl^- than to K^+.

The open probability (P_O) of the Ca^{2+}-permeable channels was dependent on the membrane potential difference (Fig. 4*C*) as shown by the sigmoidal-type of relationship. The P_O began to increase between −160 and −170 mV and reached its highest value between −180 to −190 mV.

Single-channel currents, recorded in the presence of

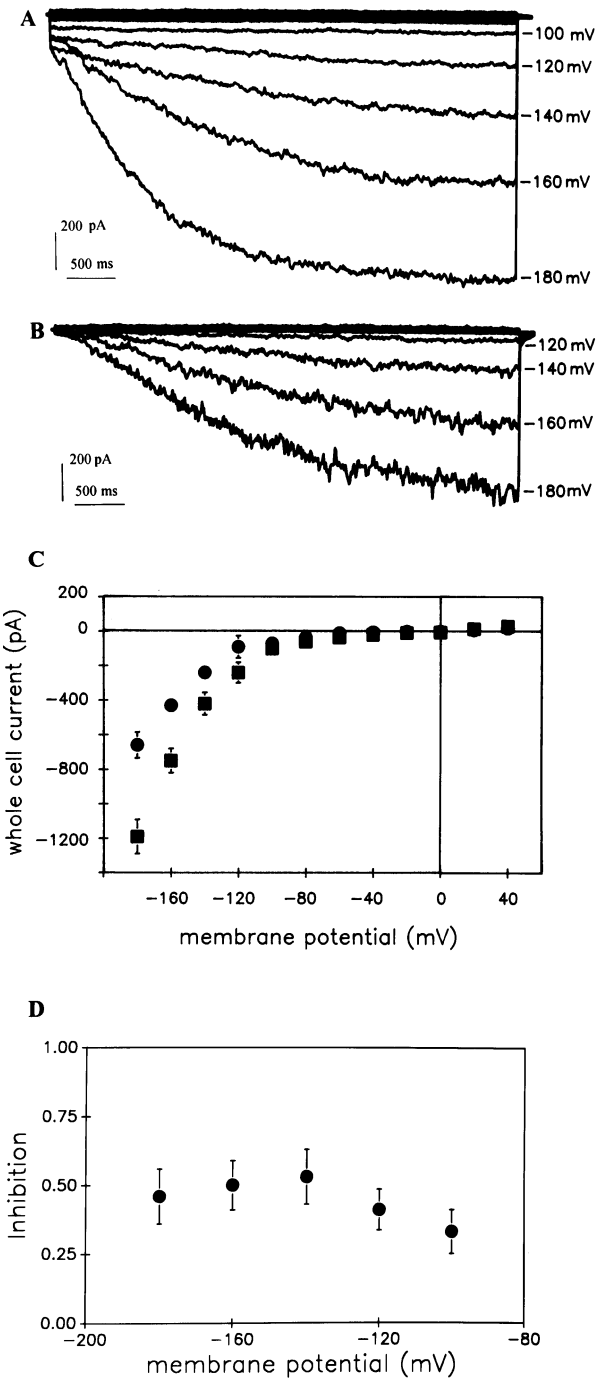

Fig. 3. Inhibition of Ba^{2+} currents by nifedipine. Time- and voltage-dependent currents (*A*) were approximately 50% inhibited (*B*) when protoplasts were exposed to 100 μM nifedipine. This inhibition was observed irrespective of the divalent cation used in the bathing solution. (*C*) Current-voltage plot from protoplasts in *A* (■) and *B* (●). Current levels measured at 4.8 sec from the onset of the imposed voltage as described in Fig. 1 were plotted against their respective voltage. Values are Mean ± SD (n = 12). (*D*) The fraction of current (measured from whole-cell recordings as shown in *A* and *B*) inhibited by nifedipine was plotted as a function of membrane voltage. Values are Mean ± SD (n = 12).

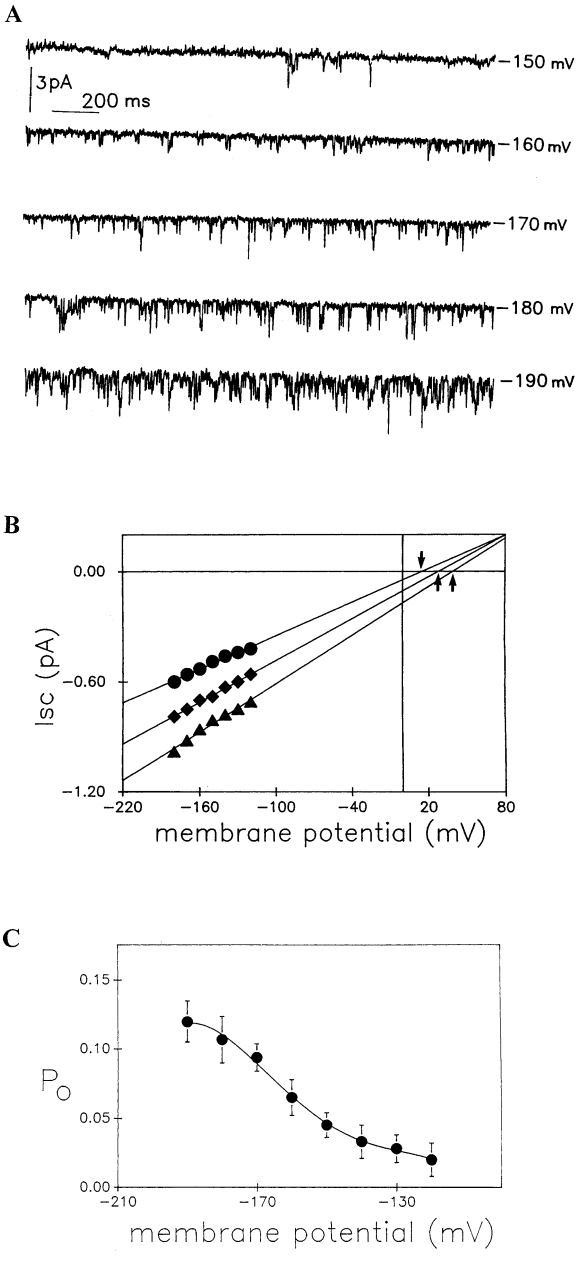

Fig. 4. Voltage-dependent single-channel currents with Ca^{2+} as the charge carrier. (*A*) Single-channel recordings of outside-out patches of membrane from protoplasts exposed to 50 mM Ca^{2+} and polarized from membrane voltages of −150 to −190 mV. Downward deflections indicate 1 or 2 channels open and correspond to the movement of Ca^{2+} into the cytosol. (*B*) Current-voltage plots from single-channel recordings similar to those shown in *A*. Channel currents were measured over a range of extracellular Ca^{2+} concentrations: 5 (●), 20 (■) and 50 mM (▲). Single-channel currents (I_{SC}) reversed (E_{rev}) direction at 14, 30 and 42 mV (indicated by arrows) as determined from a least-squares fit. Data points are Mean ± SD ($n = 8$). Error bars are smaller than size of symbols. (*C*) The open probability (P_O) of the channel is voltage-dependent. The channel P_O increased as the membrane voltage was made more negative and it reached its highest value between −180 to −190 mV.

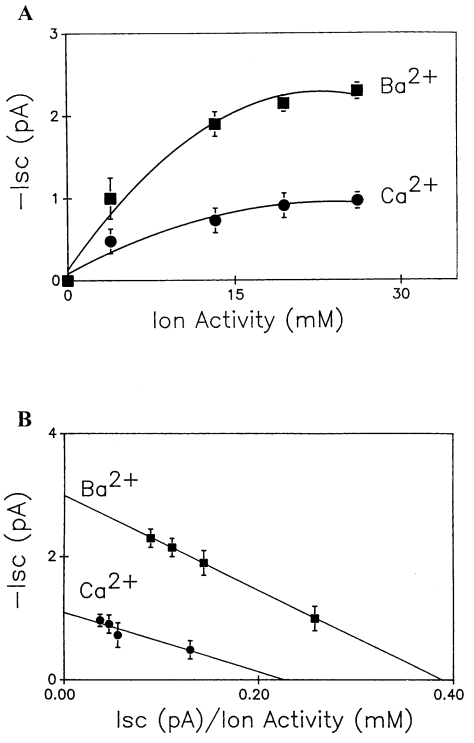

Fig; 5 The dependence of single-channel currents on the activity of Ba^{2+} and Ca^{2+}. Channel currents were measured from single-channel recordings similar to those in Fig. 4*A*. (*A*) Single-channel currents (I_{sc}) recorded at -180 mV were plotted against divalent ion activities in (mM): 3.9, 13.3, 19.5 and 26.1. Channel currents saturate with increasing concentrations of the divalent ions. (*B*) An Eadie-Hofstee plot of experimental data in *A* gave K_d values of 4.7 and 7.7 mM and single-channel maximum currents of 1.1 and 2.9 for Ca^{2+} and Ba^{2+}, respecively. Values are ± SD ($n = 8$).

increasing concentrations of extracellular Ca^{2+} and Ba^{2+}, (5, 20, 35 and 50 mM) were plotted against the activities (3.9, 13.3, 19.5 and 26.1 mM) of the divalent cations (Fig. 5*A*). Current amplitudes were obtained from single-channel records similar to those shown in Fig. 4. The currents displayed an apparent saturation with increasing activity of Ca^{2+} and Ba^{2+}. These current amplitudes were used to generate an Eadie-Hofstee plot (Fig. 5*B*) from which K_d values of 4.7 and 7.4 mM and maximum current values of 1.1 pA and 2.9 pA for Ca^{2+} and Ba^{2+}, respectively, were obtained.

Single-channel currents, recorded in the presence of 20 mM Ca^{2+} or 20 mM Ba^{2+}, resulted in two different levels of current amplitude when the membrane potential difference was maintained at −180 mV (Fig. 6). The unitary conductance decreased from 11 pS to 4 pS when Ba^{2+} was replace by Ca^{2+}. The current-voltage relationship was ohmic for both divalent cations (Fig. 6*C*). Least squares analysis resulted in reversal potentials of 26 mV (Ba^{2+}) and 30 mV (Ca^{2+}) suggesting that

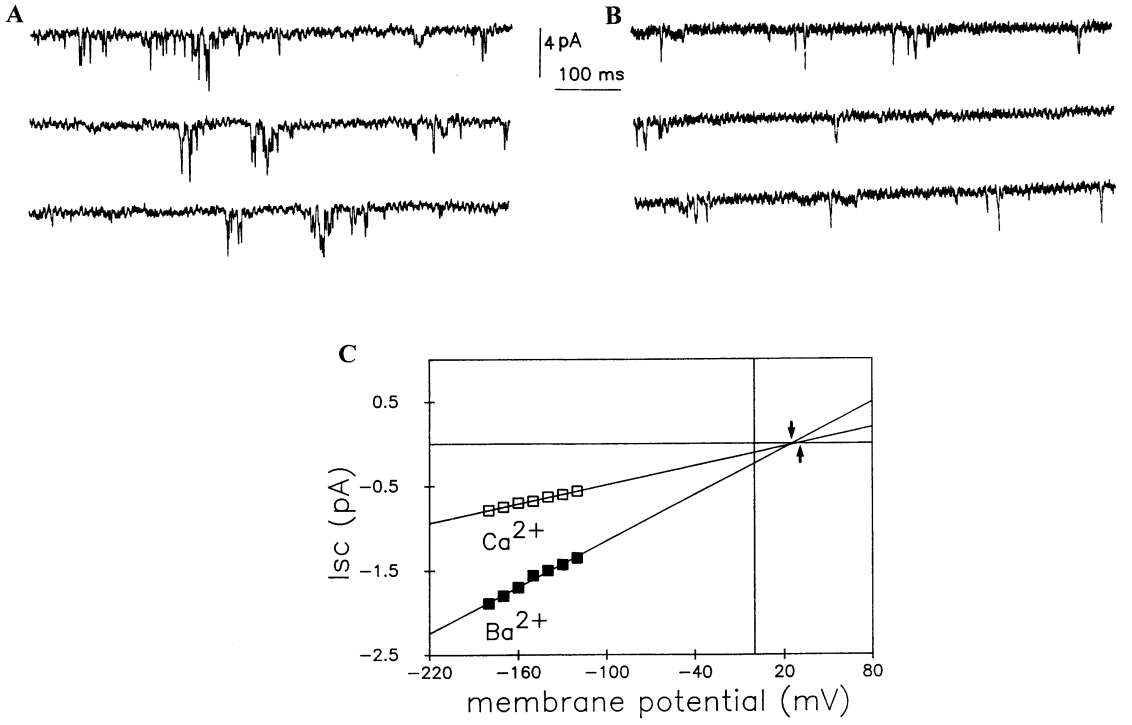

Fig. 6. Single-channel activity with Ba^{2+} and Ca^{2+} as the charge carrier. Channel recordings were obtained while polarizing the membrane to -180 mV in athe presence of 20 mM Ba^{2+} or Ca^{2+}. (*A*) With Ba^{2+} as the charge carrier, single channel current amplitude was -2.0 pA at -180 mV. At least two channels were present in the patch of membrane. (*B*) With Ca^{2+} as the charge carrier, single channel current amplitude was much smaller (-0.8 pA at -180 mV) and fewer channel events were observed. At least two channels were present in the patch of membrane. (*C*) Current-voltage relationship of single channels is linear for both Ba^{2+} and Ca^{2+}. Largest current amplitudes were observed at increasingly negative membrane voltages. Least-squares analysis gave reversal potentials (E_{rev}) of 26 and 39 mV (indicated by arrows) for Ba^{2+} and Ca^{2+}, respectively. Values are Mean ± SD (*n = 8).*

these channels are similarly permeable to Ba^{2+} and Ca^{2+} ($P^{2+}_{Ba} \approx P^{2+}_{Ca}$).

Inhibition of Single-Channel Currents by La^{3+}

Among the transition heavy metals, Al^{3+}, Gd^{3+}, La^{3+} and Zn^{2+} have been shown to block Ca^{2+}-permeable channels in both animal cells (Hille, 1992) and plant cells (Johannes, Brosnan & Sanders, 1992; Gelli & Blumwald, 1993). The concentrations used to effectively block these channels have ranged from 0.5 to 20 mM (Hille, 1993). Here, single channel currents, recorded in the presence of 50 mM Ca^{2+} while clamping the membrane voltage from −160 to −180 mV (Fig. 7*A*), were blocked by exposing the patch of membrane to 10 μM of La^{3+} (Fig. 7*C*). Similar results were observed in the presence of Ba^{2+} (*data not shown*). The frequency of channel events (Fig. 7*A*) was greatly reduced by La^{3+} (Fig. 7*C*). The inhibition of channel activity was further demonstrated by the amplitude histograms constructed from single-channel recordings (−180 mV) similar to those shown in the absence (Fig. 7*B*) and the presence of La^{3+} (Fig. 7*D*). The absence of the peak (amplitude = −1 pA) (Fig. 7*D*) corresponding to the opening of one channel is evident upon comparison (Fig. 7*D*).

Single-channel recordings obtained in the presence of 50 mM Ca^{2+} while clamping the membrane voltage to −180 mV, were used in constructing open (Fig. 8*A*) and closed time histograms (Fig. 8*B*). Both histograms were fitted with one exponential suggesting the presence of at least one closed (or one open) state of the channel (Fig. 8). The mean open and mean closed time of the channel were voltage-dependent (Fig. 8*C*). The mean closed time constants decreased while the mean open time constants increased with increasingly negative membrane voltages.

Discussion

The Voltage-Dependency of Hyperpolarization-Activated Ca^{2+} Currents

The large electrochemical potential gradient (200 to 300 mV) for calcium ions across the plasma membrane, directed into the cytosol, allows for signal amplification by

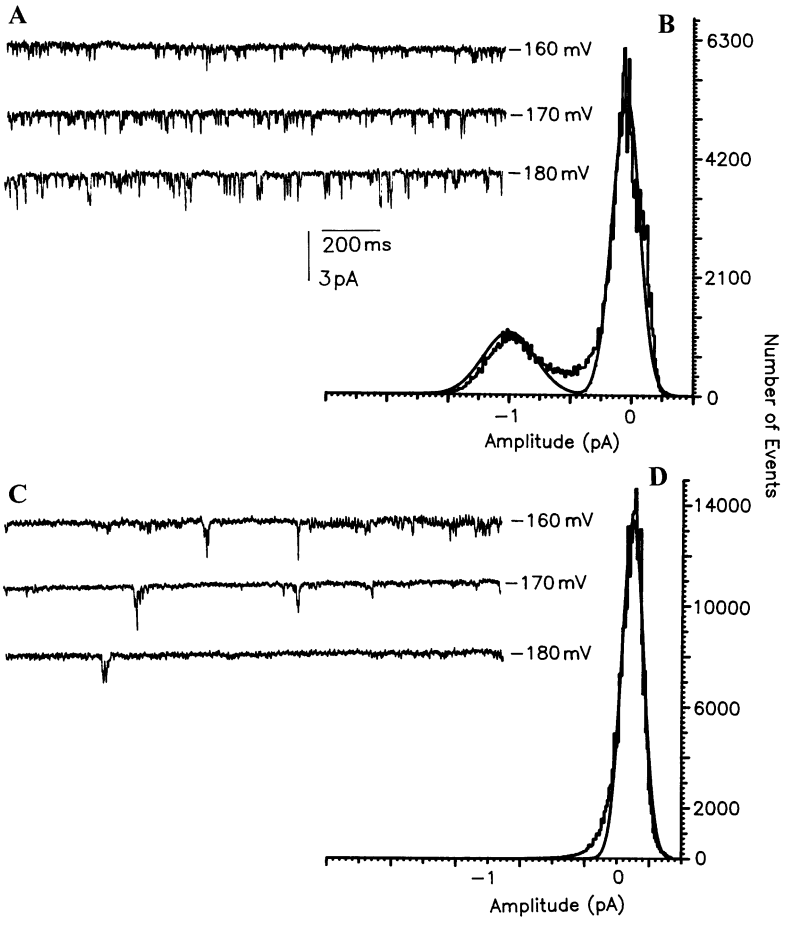

Fig. 7. Inhibition of channel activity by La^{3+}. (*A*) Voltage-dependent single-channel currents recorded in the presence of 50 mM Ca^{2+}. The number of channel events increased as the membrane voltage became increasingly negative. At least two channels were present in the patch of membrane. (*B*) Amplitude distribution histogram from single-channel recordings (-180 mV) similar to thoses show in *A*. The largest peak (0 pA) repesents the channel in the closed state. The additional peak at -1 pA corresponds to the opening of one channel. (*C*) Inhibition of single-channel activity recorded in the presence of 10 μM La^{3+}. Channel activity was significantly inhibited as demonstrated by the reduced number of channel events. (*D*) Amplitude distribution histogram from single-channel recordings similar to those shown in *C*. Inhibition of channel activity is demonstrated by the absence of the peak corresponding to the opening of one channel. Similar results were observed in six other protoplasts.

transducing an imposed signal into a controlled increase of cytosolic calcium (Bush, 1995). The localized signal perception at the plasma membrane can result in the hyperpolarization of the membrane potential from the normal range of resting potentials (Shimazaki et al., 1980; Assmann et al., 1985; Marre, 1985; Serrano et al., 1988; Felle, 1988). Plasma membrane hyperpolarization has been inferred through the activation of the tomato plasma membrane H^+-ATPase by fungal elicitors (Vera-Estrella et al., 1994). Previous work with tomato *Cf5* cell suspension cultures showed that treatment with intracellular fluids containing the *avr5* fungal elicitor led to a guanine nucleotide binding protein (G-protein)-mediated dephosphorylation of the host-plasma membrane H^+-ATPase. This resulted in the stimulation of the H^+-pump activity with the concomitant hyperpolarization of the electrical potential difference across the plasma membrane and the acidification of the extracellular milieu (Vera-Estrella et al., 1994). Thus, the activation of calcium-permeable channels at hyperpolarized membrane potentials could provide a pathway for the influx of calcium into the host cells in response to pathogen infection. The subsequent elevation of cytosolic-free calcium concentration could activate signal transduction pathways linking the perception of signals (i.e., fungal elicitors) at the host plasma membrane to the induction of a series of biochemical responses (defense responses) that are essential to the survival of the infected cell (Xing et al., 1996).

Although most of the studies on Ca^{2+} permeation through the plant plasma membrane have shown the activation of Ca^{2+}-permeable channels at depolarized potentials (Schroeder & Hagiwara, 1990; Fairely-Grenot & Assmann, 1992; White, 1994; Huang et al., 1994; Thuleau et al., 1994; Marshall et al., 1994; Piñeros & Tester, 1995), a few studies have shown Ca^{2+} influx at hyperpolarized potentials (Stoeckel & Takeda, 1995). Stoeckel and Takeda (1995) demonstrated that the delayed outward-rectifying K^+ currents in pulvinar protoplasts were reduced by increased cytosolic Ca^{2+} levels that correlated with Ca^{2+} influx at hyperpolarized potentials. The hyperpolarization-associated rundown in the K^+ outward current was reversibly blocked by La^{3+} (2 mM) and Gd^{3+} (0.5 to 2.0 mM) and it was reversed by lowering external Ca^{2+} or polarizing the membrane to less negative membrane potentials. These results suggested the operation of Ca^{2+}-permeable channels at hyperpolarized membrane potentials.

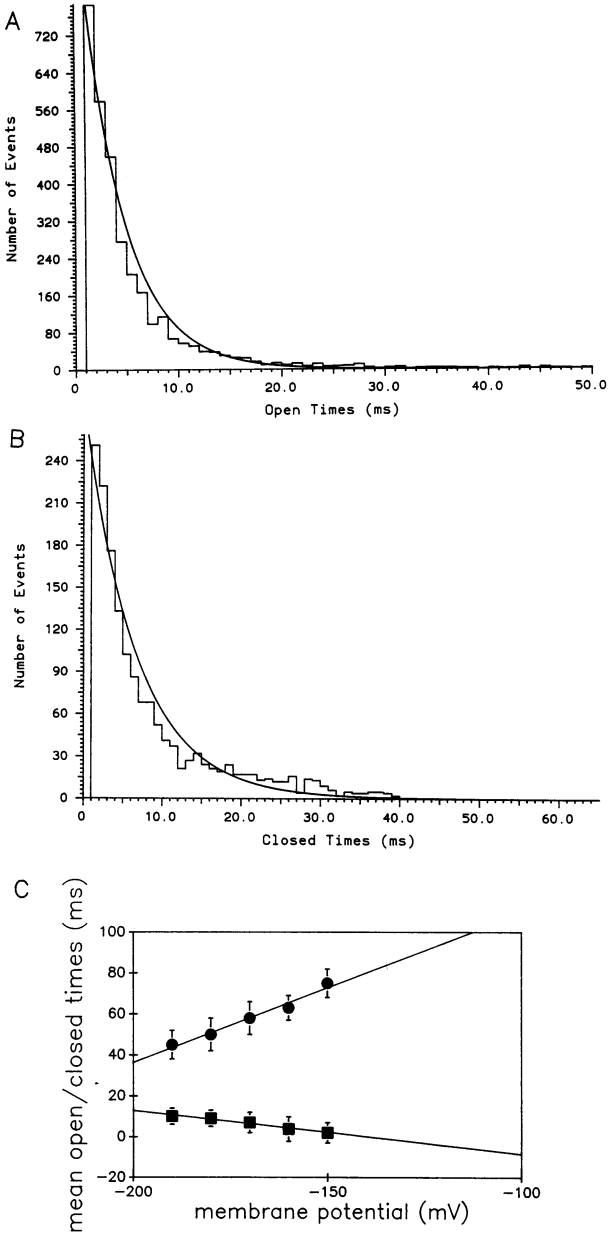

Fig. 8. Dwell time distribution histograms of the Ba^{2+} and Ca^{2+}-permeable channel. Open and closed time histograms were constructed from single-channel currents recorded at -180 mV similar to those shown in Figs. 4, 6 and 7. (*A*) Open and closed time (*B*) histograms from single-channel curents recorded in the presence of Ca^{2+} were fitted by one exponential. Events shorter than 1 msec were omitted from the fit. (*C*) The mean open and mean closed times were determined as described in Materials and Method and plotted against the applied membrane voltages. Both the mean open and mean closed times varied linearly with membrane voltage. Values are Mean ± SD ($n = 8$).

Although a full characterization of these channels has yet to be done, it is likely that the Ca^{2+} influx reported by Stoeckel and Takeda (1995) and those described here, are different from the putative depolarization-activated Ca^{2+} influx previously reported. The existence of hyperpolarization- and depolarization-activated Ca^{2+}-permeable channels may allow plant cells to efficiently couple the perception of stimuli at the plasma membrane to fluctuations in cytosolic Ca^{2+} concentrations.

The Ca^{2+}-permeable channels reported here are active at electrical membrane potential differences more negative than −120 mV (−120 to −190 mV) and become much less active upon depolarizing the membrane where the electrochemical driving force for Ca^{2+} influx is reduced. Thus the influx of Ca^{2+} into the cytosol is a voltage-dependent process. Furthermore, the Boltzman relationship for the whole cell currents revealed that channel openings (the transition from the closed state to the open state) are associated with the movement of a gating charge ($z = 1.09$) suggesting that the currents are sensitive to the electric field across the membrane, thus they are voltage-dependently gated. It is very unlikely that the inward rectifying Ca^{2+} currents are due to a Goldman-style nonlinear diffusion through an open channel that could arise when a steep gradient of ions exists across the membrane (Hille, 1992).

Selectivity and Inhibition of the Ca^{2+}-permeable Channels

The single-channel conductance suggested that Ba^{2+} (11 pS) and Ca^{2+} (4 pS) permeated the channel pore slowly, however the apparent permeabilities and the apparent K_d values suggested that both ions interacted strongly with the channel pore. Reversal potentials of the single-channel currents suggested a comparable selectivity between Ba^{2+} and Ca^{2+} although the apparent K_d values suggested a somewhat higher binding affinity for Ca^{2+} (4.7 mM) over Ba^{2+} (7.7 mM). The channels reported here were about 25 times more permeable to Ca^{2+} than to K^+ under ionic conditions of 100 mM K^+ and 100 nM Ca^{2+} in the cytosol and 0.1 mM K^+ and 5 to 50 mM Ca^{2+} in the extracellular space. This value of selectivity is comparable to that reported for the Ca^{2+} channel in the vacuolar membrane (Johannes et al., 1992; Gelli & Blumwald, 1993) and it falls in the range (3–26) of the selectivity ratios reported for the depolarization-induced Ca^{2+} channels (White, 1994; Thuleau et al., 1994; Piñeros & Tester, 1995).

Further characterization of the hyperpolarization-activated channels was attempted by examining the effect of channel blockers on whole cell and single channel currents. A series of organic (1,4-dihydropyridines including nifedipine) and inorganic (transition metals including La^{3+}) blockers have been used in the characterization of calcium channels in animal and plant systems. However the response of Ca^{2+} channels to these blockers

is variable when applied at high concentrations because of nonspecific effects (Hille, 1992; Terry, Findlay & Tyerman, 1992; Wegner et al., 1994). In several studies, La^{3+} and dihydropyridines have shown a moderate inhibition of outward-rectifying K^+ channels in the range of 10 μM to 100 μM (Terry et al., 1992) and a stronger inhibition of inward-rectifying K^+ channels at concentrations greater than 1 mM (Wegner et al., 1994). In *Chara*, La^{3+} was effective in blocking action potentials irreversibly but also blocked K^+ and Cl^- channels (Tyerman, Findlay & Paterson, 1986; Smith, Walker & Smith, 1987). Although these studies suggested that these blockers may not be highly specific for Ca^{2+} channels, more specific type of blockers have yet to be developed. Here in this study, Ca^{2+}-permeable channels were significantly inhibited by 10 μM La^{3+} and 50% inhibited by 100 μM nifedipine. The block by La^{3+} appeared to be voltage-dependent since fewer channel events were observed as the electrical membrane potential difference became more negative, suggesting that La^{3+} was bound to the channel within the electric field of the membrane. The inhibition of whole cell currents by nifedipine was not voltage-dependent.

The Physiological Role of Hyperpolarization-activated Ca^{2+}-Permeable Channels

Although not fully characterized, a few reports have described hyperpolarization-activated cation channels that could provide a pathway for the influx of Ca^{2+} (Terry, Tyerman & Findlay, 1991; Cosgrove & Hedrich, 1991; Fairley et al., 1991; Stoeckel & Takeda, 1995). The single-channel conductance ranged from 10 pS (Cosgrove & Hedrich, 1991) to 20 pS (Fairley et al., 1991), channels were weakly selective for Ca^{2+} and K^+ ($P_{Ca^{2+}}/P_{K^+} \approx 1$) (Cosgrove & Hedrich, 1991) and Cl^- ($P_{K^+}/P_{Cl^-} \approx 0.43$ (Fairley et al., 1991) and channels were inhibited by 1 mM La^{3+} (Stoeckel & Takeda, 1995).

The tomato plasma membrane Ca^{2+}-permeable channels have a characteristically small conductance (4 pS for Ca^{2+} and 11 pS for Ba^{2+}) with a higher selectivity for divalent cations ($P^{2+}_{Ca}/P^{+}_{K} \cong 20–25$, $P^{-}_{Cl}/P^{+}_{K} \cong 2$, $P^{2+}_{Ca}/P^{-}_{Cl} \cong 10–13$). It is unlikely that these hyperpolarization-activated currents are mediated through the K^+ inward rectifier (Schroeder, Raschke & Neher, 1987). Although Ca^{2+} ions can permeate the K^+ inward rectifier in guard cells (Fairley-Grenot & Assmann, 1992) and in xylem parenchyma cells (Wegner et al., 1994), these K^+ channels are strongly inhibited by Ba^{2+} ions (K_i of 1.3 mM) (Wegner et al., 1994). It has been suggested that Ba^{2+} ions can permeate K^+ channels, but so sluggishly that they effectively block the pore (Armstrong & Taylor, 1980). Tomato plasma membrane channels were permeated by Ba^{2+} with a comparable permeability to that observed with Ca^{2+}, suggesting that the channels mediating the hyperpolarization-induced Ca^{2+} currents are different from the K^+ inward rectifier.

In conclusion, the hyperpolarization-activated plasma membrane currents described in this report provide a mechanism for the influx of Ca^{2+} into tomato cells. The hyperpolarization of the electrical potential difference across the plasma membrane during pathogen attack would activate these channels allowing the influx of Ca^{2+} into the host cell. The subsequent elevation of cytosolic Ca^{2+} serves to activate signal transduction pathways that link the perception of fungal elicitors at the plasma membrane to the induction of plant defense responses (Xing et al., 1996). The hyperpolarization-induced increase in cytosolic Ca^{2+} concentration is currently being quantified and mechanisms of Ca^{2+} influx regulation are being investigated.

References

Allen, G.I., Sanders, D. 1994. Two voltage-gated, calcium release channels coreside in the vacuolar membrane of broad bean guard cells. *Plant Cell* **6:**685–694

Armstrong, C.M., Taylor, S.R. 1980. Interaction of barium ions and potassium channels. *Biophys. J.* **30:**473–488

Assmann, S.M., Simoncini, L., Schroeder, J.L. 1985. Blue light activates electrogenic ion pumping in guard cell protoplasts in *Vicia faba* L. *Nature* **318:**285–287

Barry, P.H., Lynch, J.W. 1991. Liquid junction potentials and small cell effects in patch clamp analysis. *J. Membrane Biol.* **121:**101–117

Bush, D.S. 1993. Regulation of cytosolic calcium in plants. *Plant Physiol.* **103:**7–13

Catteral, W.A., Striessnig, J. 1992. Receptor sites for Ca^{2+} channel antagonists. *Trends Pharmacol. Sci.* **13:**256–262

Cosgrove, D.J., Hedrich, R. 1991. Stretch-activated chloride, potassium and calcium channels coexisting in plasma membranes of guard cells of *Vicia faba* L. *Planta* **186:**143–153

Ding, J.P., Pickard, B.G. 1993. Mechanosensory calcium-selective cation channels in epidermal cells. *Plant J.* **3:**83–110

Ebel, J., Cosio, E.G. 1994. Elicitors of plant defense responses. *Int. Rev. Cytol.* **148:**1–36

Fairley, K., Laver, D., Walker, N.A. 1991. Whole-cell and single channel currents across the plasmalemma of corn shoot suspension cells. *J. Membrane Biol.* **121:**11–22

Fairley-Grenot, K., Assmann, S.M. 1992. Permeation of Ca^{2+} through K^+ channels in the plasma membrane of *Vicia faba* guard cells. *J. Membrane Biol.* **128:**103–113

Felle, H. 1988. Auxin causes oscillation of cytosolic free calcium and pH in *Zea mays* L. coleoptiles. *Planta* **174:**495–499

Gelli, A., Blumwald, E. 1993. Calcium retrieval from vacuolar pools. Characterization of a vacuolar calcium channel. *Plant Physiol.* **106:**1139–1146

Hamill, O.P., Marty, A., Neher, E., Sakmann, E., Sigworth, F.J. 1981. Improved patch-clamp techniques for high-resolution current recordings from cells and cell-free membrane patches. *Pfluegers Arch.* **391:**85–100

Hayama, T., Shimmen, T., Tazawa, M. 1979. Participation of Ca^{2+} in cessation of cytoplasmic streaming induced by membrane excitation in *Characeae* internodal cells. *Protoplasma* **99:**305–321

Hille, B. 1992. Ionic channels of excitable membranes. 2nd edition. Sinauer, Sunderland, MA

Huang, J.W., Grunes, D.L., Kochian, L.V. 1994. Voltage-dependent Ca^{2+} influx into right-side-out plasma membrane vesicles isolated from wheat roots: Characterization of a putative Ca^{2+} channel. *Proc. Natl. Acad. Sci. USA* **91:**3473–3477

Johannes, E., Brosnan, J.M., Sanders, D. 1992. Parallel pathways for intracellular Ca^{2+} release from the vacuole of higher plants. *Plant J.* **2:**97–102

Labarca, P., Coronado, R., Miller, C. 1980. Thermodynamic and kinetic studies of the gating behavior of a K^+-selective channel from the sacroplasmic reticulum membrane. *J. Gen. Physiol.* **76:**397–424

Lewis, C.A. 1979 Ion-concentration dependence of the reversal potential and the single channel conductance of ion channels at the from neuromuscular junction. *J. Physiol.* **286:**417–445

Lohse, G., Hedrich, R. 1992. Characterization of the plasma membrane H^+-ATPase from *Vicia faba* guard cells. *Planta* **188:**206–214

Lunevsky, V.Z., Zherelova, O.M., Vostrikov, M.G., Berestovksy, G.N. 1983. Excitation of *Characeae* cell membranes as a result of activation of calcium and chloride channels. *J. Membrane Biol.* **72:**43–58

Marre, E. 1985. Fusicoccin- and hormone-induced changes of H^+ extrusion: Physiological implications. *In:* Frontiers of membrane research in agriculture. St. John, E. Berlin, P. Jackson, eds. pp. 439–460. Rownan and Allanheld, Ottawa

Marshall, J., Corzo, A., Leigh, R.A., Sanders, D. 1994. Membrane potential-dependent calcium transport in right-side-out plasma membrane vesicles from *Zea mays* L. roots. *Plant J.* **5:**683–694

Nobel, P.S. 1991. The Debey-Hückel formula for the activity coefficient. *In:* Physicochemical and environmental plant physiology, pp. 114–116. Academic Press, CA

Piñeros, M., Tester, M. 1995. Characterization of a voltage-dependent Ca^{2+}-selective channel from wheat roots. *Planta* **195:**478–488

Plant, P.J., Gelli, A., Blumwald, E. 1994. Vacuolar chloride regulation of an anion selective tonoplast channel. *J. Membrane Biol.* **140:**1–12

Schroeder, J.I., Hagiwara, S. 1990. Repetitive increase in cytosolic Ca^{2+} of guard cells by abscisic acid activation of nonselective Ca^{2+} permeable channels. *Proc. Natl. Acad. Sci. USA* **87:**9305–9309

Schroeder, J.L., Raschke, K., Neher, E. 1987. Voltage-dependence of K^+ channels in guard cell protoplasts. *Proc. Natl. Acad. Sci. USA* **4:**4108–4112

Schwacke, R., Hager, A. 1992. Fungal elicitors induce a transient release of active oxygen species from cultured spruce cells that is dependent on Ca^{2+} and protein-kinase activity. *Planta* **187:**136–141

Serrano, E.E., Zeiger, E., Hagiwara, S. 1988. Red light stimulates an electrogenic proton pump in *Vicia faba* L. guard cell protoplasts. *Proc. Natl. Acad. Sci. USA* **85:**436–440

Shimazaki, K.I., Kinoshita, T., Nishimura, M. 1992. Involvement of Calmodulin and Calmodulin-dependent myosin light chain kinase in blue light-dependent H^+ pumping by guard cell protoplasts from *Vicia faba* L. *Plant Physiol.* **99:**1416–1421

Smith, J.R., Walker, N.A., Smith, F.A. 1987. Potassium transport across the membranes of *Chara.* III. Effects of pH, inhibitors and illumination. *J. Exp. Bot.* **38:**778–787

Stoeckel, H., Takeda, K. 1995. Calcium-sensitivity of the plasmalemmal delayed rectifier potassium current suggests that calcium influx in pulvinar protoplasts from *Mimosa pudica* L. can be revealed by hyperpolarization. *J. Membrane Biol.* **146:**201–209

Terry, B.R., Tyerman, S.D., Findlay, G.P. 1991. Ion channels in the plasma membrane of *Amaranthus* protoplasts: One cation and one anion channel dominate the conductance. *J. Membrane Biol.* **121:**223–236

Terry, B.R., Findlay, G.P., Tyerman, S.D. 1992. Direct effects of Ca^{2+} channel blockers on plasma membrane cation channels of *Amarantus tricolor* protoplasts. *J. Exp. Bot.* **256:**1457–1473

Thuleau, P., Ward, J.M., Ranjeva, R., Schroeder, J.L. 1994. Voltage-dependent calcium-permeable channels in the plasma membrane of higher plant cells. *EMBO J.* **13:**2970–2975

Tsien, R.Y. 1980. New calcium indicators and buffers with high selectivity against magnesium and protons: Design, synthesis and properties of prototype structures. *Biochem.* **19:**2396–2403

Tyerman, S.D., Findlay, G.P., Paterson, G.J. 1986. Inward membrane current in *Chara inflata;* II Effects of pH, Cl^- channel blockers and NH^{4+} and significance for the hyperpolarized state. *J. Membrane Biol.* **89:**153–161

Ullrich, C.I., Novacky, A.J. 1991. Electrical membrane properties of leaves, roots and single-cap cells of susceptible *avena sativa. Plant Physiol.* **95:**675–681

Vera-Estrella, R., Barkla, B., Higgins, V.J., Blumwald, E. 1994. Plant defense responses to fungal pathogens. Activation of host-plasma membrane H^+-ATPase by elicitor-induced enzyme dephosphorylation. *Plant Physiol.* **104:**209–215

Wegner, L.H., De Boer, A.H., Raschke, K. 1994. Properties of the K^+ inward rectifier in the plasma membrane of xylem parenchyma cells from barley roots: Effects of TEA^+, Ca^{2+}, Ba^{2+} and La^{3+}. *J. Membrane. Biol.* **142:**363–379

White, P.J. 1994. Characterization of a voltage-dependent cation-channel from the plasma membrane of rye (*Secale cereale* L.) roots in planar lipid bilayers. *Planta* **193:**186–193

Xing, T., Higgins, V.J., Blumwald, E. 1996. Regulation of plant defense responses to fungal pathogens: Two types of protein kinases in the reversible phosphorylation of the host plasma membrane H^+-ATPase *Plant Cell* **8:**555–564